Mutations at the Histidine 249 Ligand Profoundly Alter the Spectral and Iron-Binding Properties of Human Serum Transferrin N-Lobe†

Qing-Yu He,*,‡ Anne B. Mason,‡ Rowchanak Pakdaman,§ N. Dennis Chasteen,§ Bonnie K. Dixon,‡ Beatrice M. Tam,|| Vinh Nguyen,|| Ross T. A. MacGillivray,|| and Robert C. Woodworth‡

Department of Biochemistry, College of Medicine, University of Vermont, Burlington, Vermont 05405, Department of Chemistry, Parsons Hall, University of New Hampshire, Durham, New Hampshire 03824, and Department of Biochemistry and Molecular Biology, University of British Columbia, Vancouver, BC V6T 1Z3, Canada

Received July 1, 1999; Revised Manuscript Received September 28, 1999

ABSTRACT: Human serum transferrin is an iron-binding and -transport protein which carries iron from the blood stream into various cells. Iron is held in two deep clefts located in the N- and C-lobes by coordinating to four amino acid ligands, Asp 63, Tyr 95, Tyr 188, and His 249 (N-lobe numbering), and to two oxygens from carbonate. We have previously reported the effect on the iron-binding properties of the N-lobe following mutation of the ligands Asp 63, Tyr 95, and Tyr 188. Here we report the profound functional changes which result from mutating His 249 to Ala, Glu, or Gln. The results are consistent with studies done in lactoferrin which showed that the histidine ligand is critical for the stability of the iron-binding site [H. Nicholson, B. F. Anderson, T. Bland, S. C. Shewry, J. W. Tweedie, and E. N. Baker (1997) *Biochemistry 36*, 341−346]. In the mutant H249A, the histidine ligand is disabled, resulting in a dramatic reduction in the kinetic stability of the protein toward loss of iron. The H249E mutant releases iron three times faster than wild-type protein but shows significant changes in both EPR spectra and the binding of anion. This appears to be the net effect of the metal ligand substitution from a neutral histidine residue to a negative glutamate residue and the disruption of the "dilysine trigger" [MacGillivray, R. T. A., Bewley, M. C., Smith, C. A., He, Q.-Y., Mason, A. B., Woodworth, R. C., and Baker, E. N. (2000) *Biochemistry 39*, 1211−1216]. In the H249Q mutant, Gln 249 appears not to directly contact the iron, given the similarity in the spectroscopic properties and the lability of iron release of this mutant to the H249A mutant. Further evidence for this idea is provided by the preference of both the H249A and H249Q mutants for nitrilotriacetate rather than carbonate in binding iron, probably because NTA is able to provide a third ligation partner. An intermediate species has been identified during the kinetic interconversion between the NTA and carbonate complexes of the H249A mutant. Thus, mutation of the His 249 residue does not abolish iron binding to the transferrin N-lobe but leads to the appearance of novel iron-binding sites of varying structure and stability.

Serum transferrin belongs to a group of iron-binding proteins including lactoferrin and ovotransferrin (*1*−*3*). In vivo, the major function of transferrin is to transport iron into cells and minimize levels of free iron in body fluids. Crystal structures of human serum transferrin and a number of other transferrins reveal that these proteins consist of a single polypeptide chain folded into two lobes, representing homologous N- and C-terminal halves; each lobe contains a metal-binding site holding an Fe(III) tightly in a deep cleft between two domains (*4*−*8*). Iron binding involves distorted octahedral coordination with four amino acid ligands and two oxygens from a synergistically bound anion that is usually carbonate.

Human transferrin N-lobe (hTF/2N)[1] has been generated by means of recombinant DNA technology and has proven to be an excellent mimic for the N-terminal lobe in the full-length transferrin (*9*, *10*). Recent structural analysis has shown that, when iron is released, the two domains of hTF/2N rotate 63° around a hinge to form an open conformation (*8*, *11*). The iron-binding ligands in hTF/2N are Asp 63, Tyr 95, Tyr 188, and His 249. Previous reports have shown that mutation of the Asp 63, Tyr 95, and Tyr 188 ligands results in dramatic functional changes in the protein (*12*, *13*). As part of a series of studies on the structure−function relationships of human transferrin, the current work addresses the effect of mutation at the final ligand, His 249. To this end, three single-point mutant proteins in which His 249 was

†This work was supported by USPHS Grant R01-DK-21739 from the National Institute of Diabetes, and Digestive and Kidney Diseases and shared instrumentation Grant 1-S10-RR12926-01 from National Center for Research Resources (to R.C.W.) and grant R37-GM-20194 from the National Institute of General Medical Sciences (to N.D.C.). Q.-Y. H. was supported by a Postdoctoral Fellowship from the American Heart Association, ME/NH/VT Affiliate.

* To whom correspondence should be addressed. Phone: (802) 656-0343. Fax: (802) 862-8229. E-mail: qhe@zoo.uvm.edu.

‡ University of Vermont.

§ University of New Hampshire.

|| University of British Columbia.

[1] Abbreviations: hTF/2N, recombinant N-lobe of human transferrin comprising residues 1−337; mutants of hTF/2N are designated by the wild-type amino acid residue, the sequence number and the amino acid to which the residue was mutated; BHK, baby hamster kidney cells; NTA, nitrilotriacetate; EDTA, ethylenediaminetetraacetate; Tiron, 4,5-dihydroxy-1,3-benzenedisulfonate; EPR, electron paramagnetic resonance.

10.1021/bi9915216 CCC: $19.00
Published on Web 01/12/2000

changed to Glu, Gln, or Ala have been expressed and purified. The iron-binding properties of the three mutants have been comprehensively investigated by means of UV−vis and EPR spectroscopies, anion-binding titration, and the kinetics of iron uptake and iron release. The characteristics of the histidine mutants are compared to the parent N-lobe and to the other mutants in which a ligand has been disrupted.

MATERIALS AND METHODS

Materials. Chemicals were of reagent grade. Stock solutions of Hepes, Mes, and other buffers were prepared by dissolving the anhydrous salts in Milli-Q (Millipore) purified water, and adjusting the pH to desired values with 1 N NaOH or HCl. 4,5-Dihydroxy-1,3-benzenedisulfonate (Tiron) came from Fisher Scientific Co., ethylenediaminetetraacetate (EDTA) from Mann Research Laboratories, Inc., and nitrilotriacetate (NTA) from Sigma. Centricon 10 microconcentrators were from Amicon. Tiron and EDTA stock solutions were prepared by dissolving these chelators in the appropriate buffers and adjusting the pH to the desired values with 1 and 10 M NaOH. No chloride is in the stock solutions.

Molecular Biology. Mutation of His 249 to alternative amino acids was carried out by using a polymerase chain reaction (PCR) based mutagenesis procedure (*14*). The following synthetic oligonucleotides were used to introduce the mutations:

H249A: 5′-TCCCTTCTGCGACCGTCGTGG-3′

H249E: 5′-GGTCCCTTCTGAAACCGTCGTGG-3′

H249Q: 5′-TCCCTTCTCAGACCGTCGTGG-3′

A protocol similar to that described previously in detail was employed to confirm the presence of the desired mutation and to place the mutagenized hTF/2N into the pNUT vector (*12*, *15*, *16*).

Expression, Purification, and Preparation of Proteins. The N-lobe of hTF and the mutants of hTF/2N were expressed by using the pNUT-BHK cell system and purified by methods described previously (*9*, *16*, *17*). The preparation of apo- and Fe(III)-loaded protein samples followed the procedure described in detail previously (*12*). Additional treatment is required to achieve pure samples of either carbonate or NTA complexes of the H249A and H249Q mutants (see Results).

Absorption Spectra. UV−vis spectra were recorded on a Cary 219 spectrophotometer under the control of the computer program Olis-219s (On-line Instrument Systems, Inc., Bogart, GA). The appropriate buffer served as the reference for full-range spectra from 250 to 600 nm. Difference spectra were generated by storing the spectrum of the apo-protein as the baseline and subtracting it from the sample spectra.

EPR Spectra. The spectrometer and instrumental settings for measuring EPR spectra of iron transferrins have been described in detail elsewhere (*18*). All EPR spectra were obtained in 100 mM Hepes, pH 7.4, buffer containing 100 mM bicarbonate (for the carbonate complexes of proteins) or 1 mM NTA (for the NTA complexes of proteins).

Kinetics of Iron Removal. The kinetics of iron release from transferrin and the processing of the data were carried out by means of the procedure described previously (*12*, *13*, *19*). Tiron was used as the chelator for iron removal at pH 7.4, 25 °C. The data were analyzed with single-exponential functions, giving r^2 values (coefficients of determination) greater than 0.99 in all cases.

Table 1: Summary of the Spectral Characteristics for Wild-Type hTF/2N and Mutants[a]

	λ_{max} (nm)	λ_{min} (nm)	A_{max}/A_{min}	A_{280}/A_{max}
Fe-hTF/2N(WT)-CO_3	472	410	1.37	23.5
Fe-H249E-CO_3	457	400	1.30	25.3
Fe-H249A-CO_3	439 (430)	379 (385)	1.28 (1.11)	23.8 (24.6)
Fe-H249A-NTA	472	400	1.42	20.2
Fe-H249Q-CO_3	463 (442)	400 (394)	1.33 (1.13)	21.0 (22.4)
Fe-H249Q-NTA	472	400	1.38	21.7

[a] Spectra were taken in 50 mM Hepes buffer (pH 7.4). Data for wild-type hTF/2N are from He et al (*12*). Data in parentheses are for the spectra taken in the same Hepes solution containing 100 mM bicarbonate.

For iron release from the H249A and H249Q mutants (fast reaction), the kinetics was determined with an Olis-RSM 1000 stopped-flow spectrophotometer using the UV−vis absorbance module. The general settings and data processing were identical to those described previously (*16*). For the current experiments, Hepes (50 mM, pH 7.4) was used in both syringes and λ_{480nm} was selected as the central wavelength to monitor the spectral change upon iron removal by Tiron. The reported data are the average values of at least four assays.

Anion-Exchange and Iron-Uptake Kinetics. Anion-exchange and iron-uptake experiments were also performed with the Olis-RSM 1000 stopped-flow spectrophotometer in 50 mM Hepes, pH 7.4. For anion exchange, the reaction was monitored by scanning full-scale spectra (460 ± 115 nm) over time and the resulting 3D data were processed using a global-fitting function (Olis) to determine the kinetic changes of all species. The final concentrations used were 13 μM protein, 0.5 mM NTA, and 5 mM bicarbonate. Fresh NH_4HCO_3 stock solution (1 M, pH 7.6) was used as the bicarbonate source to maintain a constant final pH. For iron uptake, 470 nm was used to monitor the formation of iron complexes, Fe(III)$(NTA)_2$ was used as the iron source, and the final concentration of iron was 65 μM, which is 10 times more than the concentration of the apo-proteins used. The equilibrium concentration of bicarbonate in a pH 7.4 buffer solution is about 0.17 mM from atmospheric CO_2 (*10*), and no additional bicarbonate was added. The resulting kinetic curves were analyzed by a single-exponential function, which gave a very good fit.

Anion-Binding Titration. Anion titrations of apo-protein and the calculation of the binding constants were carried out as previously described using K_2SO_4 in the concentration range 0.04−6.0 mM (*16*, *20*). Hepes (50 mM) was used for titrations at pH 7.4; in each case, the protein concentration was approximately 13 μM.

RESULTS

Absorption Spectra. UV−vis spectra for the mutant proteins were taken from 250 to 600 nm, which covers the electronic spectral features of transferrins. Table 1 summarizes some of the intrinsic spectral parameters for the iron-saturated proteins of the three histidine mutants and wild-type hTF/2N. Both the H249A and H249Q mutants have two forms, the carbonate complex and the NTA complex.

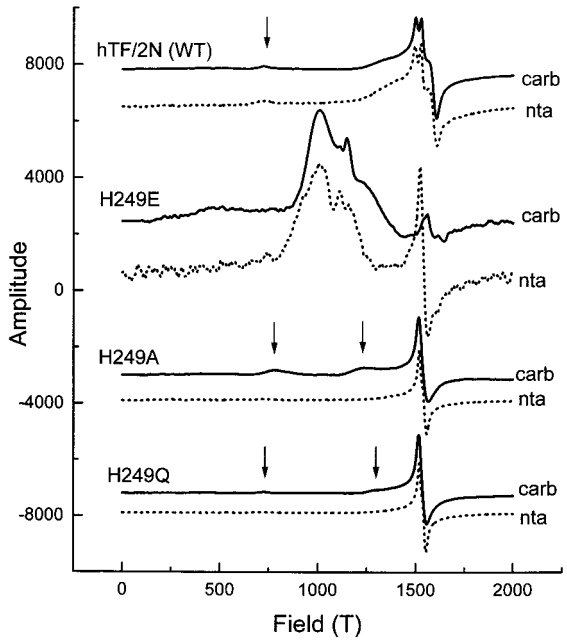

FIGURE 1: X-band (9.38 GHz) EPR spectra of frozen samples of iron-saturated wild-type hTF/2N and various histidine mutants. Protein samples (~0.4 mM), Hepes buffer (~0.1 M, pH 7.5) containing $NaHCO_3$ (~100 mM) or NTA (1 mM), temperature 90 K.

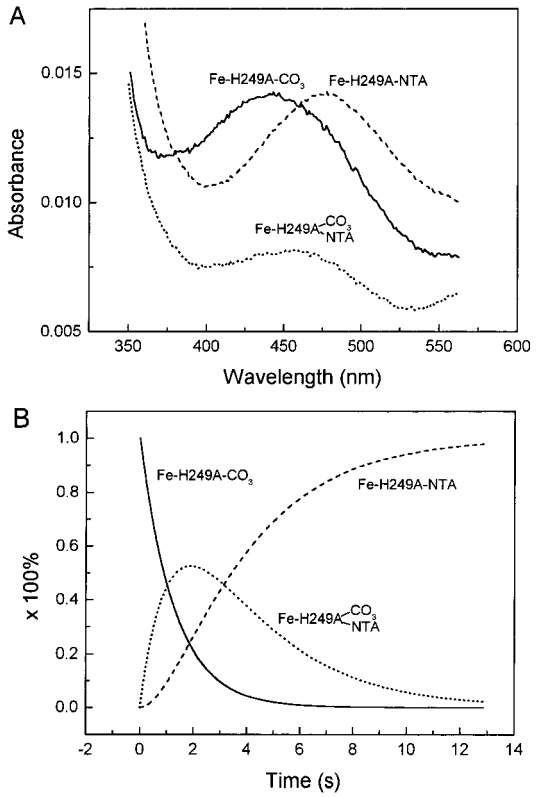

FIGURE 2: 2D full-scale spectra (A) and kinetic plot (B) showing the spectral and the kinetic changes of the three species during anion exchange reaction of the H249A mutant.

These two forms readily interconvert during protein handling, which results in mixed spectra and double-exponential iron-release curves in kinetic assays. When excess $Fe(III)(NTA)_2$ is added to either mutant apo-H249A or apo-H249Q in the absence of bicarbonate (pH 7.4), a pink ternary Fe-protein−NTA complex is formed. Exhaustive exchange into Hepes buffer containing 0.1 M bicarbonate (pH 7.4) leads to the ternary carbonate complex which is orange in color for H249Q and yellow in color for H249A. Exchange of the carbonate complex with Hepes buffer containing 1 mM NTA three times returns both proteins to the pink form. When treated as above, both the wild-type Fe-hTF/2N and the Fe-H249E mutant protein remain unchanged with regard to their UV−vis spectra, pink in color for wild-type hTF/2N, and orange in color for the mutant.

The iron-containing H249E mutant protein has a λ_{max} = 457 nm, which is blue-shifted 15 nm when compared to that (472 nm) for wild-type Fe-hTF/2N. For the mutants Fe-H249A and Fe-H249Q, the NTA complexes have similar spectral parameters to wild-type Fe-hTF/2N with slightly smaller A_{280}/A_{max} ratios, while the carbonate complexes are significantly blue-shifted with regard to λ_{max}. After the final step of purification involving passage over a gel filtration column in 0.1 M ammonium bicarbonate, the Fe-H249A mutant had a faint yellow color and an A_{280}/A_{max} ratio of ~50. When additional iron was added to the protein, the A_{280}/A_{max} ratio decreased to ~24 (Table 1), which indicated that only about half of the protein retained iron in the original bicarbonate complex.

EPR Spectra. EPR spectra for wild-type hTF/2N and the H249 mutants are shown in Figure 1. Wild-type Fe-loaded hTF/2N in both the bicarbonate- and NTA-containing solutions shows similar EPR spectra, featuring a rhombic structure with slight axial symmetry represented by three signals near $g' = 4.3$ and another small signal near $g' = 9.06$, characteristic of the carbonate complexes of the transferrins. This result indicates that the presence of NTA does not disturb the normal carbonate binding in wild-type Fe-hTF/2N. For the H249A and H249Q mutants, spectral changes are observed between the carbonate and NTA complexes. In both cases, while the pure rhombic single component signal at $g' = 4.3$ remains unchanged, two small features around $g' = 8.5$ and 5.5 (denoted by arrows in Figure 1) disappear in the EPR spectra of the NTA complexes. The EPR spectrum of the H249E mutant taken in solution containing NTA shows the appearance of a single component signal near $g' = 4.3$ due to the Fe-H249E-NTA complex, which based on double integration of the signal represents only ~6% of the total. A comparison with the $g' = 4.3$ spectrum of free $Fe(III)(NTA)_2$ in buffer alone demonstrated that the observed $g' = 4.3$ signal was not due to $Fe(III)(NTA)_2$. The bulk of the iron remains as the carbonate complex, exhibiting the broad axial EPR spectrum around $g' = 7$ and accounting for most of the EPR intensity.

Anion Exchange in H249A. An anion-exchange experiment was carried out using the H249A mutant since there is a large λ_{max} difference between the carbonate and NTA complexes. The kinetics of the reversible conversion between the two complex forms can be followed with a stopped-flow absorbance spectrometer. When the resulting 3D kinetic data were fitted with the global fitting function, three species were identified as shown in Figure 2A (full-scale 2D spectra with 460 nm as the central wavelength), indicating that an intermediate species exists. A sequential reaction X → Y → Z was selected for the fitting using 460 nm kinetic trace, generating two rate constants k_1 and k_2. The starting material becomes the intermediate with a rate constant of k_1 and the

Table 2: Rate Constants k (min^{-1}) for Iron Removal from hTF/2N and Mutants[a]

[KCl] (mM)	0	50
Fe-hTF/2N(WT)-CO_3	0.0225 ± 0.0009	0.0205 ± 0.0005
Fe-H249E-CO_3	0.0736 ± 0.0021	0.0610 ± 0.0033
Fe-H249A-CO_3	295 ± 26	499 ± 42
Fe-H249A-NTA	3.32 ± 0.10	4.49 ± 0.15
Fe-H249Q-CO_3	261 ± 11	327 ± 13
Fe-H249Q-NTA	5.95 ± 0.18	6.73 ± 0.12

[a] [Tiron] = 12 mM, [Hepes] = 50 mM, pH 7.4, 25 °C.

Table 3: Sulfate Titration to Wild-type Apo-hTF/2N and the Histidine Mutants[a]

protein	$\Delta\epsilon_{245}$ (M^{-1} cm^{-1})	K ($1/K_d$) (M^{-1})
hTF/2N (WT)	5170	5840
Apo-H249A	5280	4550
Apo-H249E		
Apo-H249Q	3910	2360

[a] [Protein] = 6.5 μM, [Hepes] = 50 mM, pH 7.4, 25 °C.

intermediate goes to the final product with a rate constant of k_2. The kinetic change for each individual species is shown in Figure 2B. When NH_4HCO_3 was added to the Fe-H249A−NTA protein, a similar but slower pattern of spectral change was found and subjected to the same method of analysis.

When a 38-fold excess of NTA (0.5 mM) was mixed with the Fe-H249A−CO_3 protein (13 μM), the carbonate complex picked up NTA rapidly to become an intermediate (k_1 = 0.719 s^{-1}) while the final product, Fe-H249A−NTA, formed at a rate about three times slower (k_2 = 0.263 s^{-1}). The reverse conversion from the NTA complex to the carbonate complex required much more bicarbonate (5 mM, 380-fold excess) to reach a similar k_1 (0.729 s^{-1}), but the k_2 (0.0176 s^{-1}) is still 15 times smaller than that for the reverse procedure.

Iron-Release Kinetics. Iron-release experiments were performed to determine the effect of the mutations on the kinetic stability of Fe-hTF/2N. Table 2 lists the rate constants for the iron removal from wild-type Fe-hTF/2N and the mutant proteins by Tiron at pH 7.4. In the absence or presence of chloride, iron release from the H249E mutant is three times faster than that from wild-type Fe-hTF/2N, and chloride exerts a similar moderate retarding effect on the iron release from both the H249E mutant and the wild-type protein. Under the same conditions, the H249A and H249Q mutants are much more labile kinetically. Iron can be easily removed from the NTA complexes of both H249A and H249Q mutants with rates about 150 and 250 times faster than that for wild-type Fe-hTF/2N. Further, in both cases, the rate constants for the iron release from the carbonate complexes are even higher, about 100 and 50 times larger than those for the corresponding NTA complexes. In contrast to results found for wild-type Fe-hTF/2N, chloride exerts a significant accelerating effect on iron release from these very weak iron-binding mutant proteins, as might be expected.

Anion Binding. In the anion-binding titration experiments, sulfate was used as a binding anion since it gives a strong absorption signal upon binding to the protein (*16*). The maximum extinction coefficient, $\Delta\epsilon_{245}$, and the binding constant K for the sulfate titration to the apo-proteins of wild-type and the histidine mutants are summarized in Table 3. Compared to the wild-type apo-hTF/2N, apo-H249A has slightly weaker sulfate binding with an essentially unchanged $\Delta\epsilon$, while apo-H249Q features a significantly weaker sulfate binding (K is 60% less) with a smaller $\Delta\epsilon$. Interestingly, sulfate titration of the apo-H249E mutant gave no measurable absorption spectra for $\Delta\epsilon$ and K; only weak featureless absorbance signals were observed, similar to the situation found with apo-K296E (*16*).

Table 4: Rate Constants k (min^{-1}) for Iron Uptake by hTF/2N[a]

[KCl] (mM)	0	50	140
hTF/2N (WT)	38.1 ± 0.6	36.2 ± 0.3	32.2 ± 0.5
H249E	30.2 ± 0.9	14.3 ± 0.6	8.60 ± 0.30
H249A	36.1 ± 1.2	34.8 ± 0.6	30.2 ± 1.6
H249Q	62.5 ± 1.4	45.1 ± 1.0	27.4 ± 1.3

[a] [Protein] = 6.5 μM, [Fe(III)$(NTA)_2$] = 65 μM, [$NaHCO_3$] ≈ 0.15 mM, [Hepes] = 50 mM, pH 7.4, 25 °C.

Iron Uptake. The kinetics of iron uptake from Fe(III)-$(NTA)_2$ by the three histidine mutants were also measured. Table 4 lists the rate constants for the iron uptake by wild-type apo-hTF/2N and the histidine mutants under three different conditions. In the absence of chloride, iron uptake is moderately slower for the H249E mutant and slightly slower for H249A compared to wild-type protein. In contrast, the H249Q mutant rapidly acquires iron with a rate which is about double that found for the other proteins. Overall, chloride retards the iron uptake for both wild-type apo-hTF/2N and the apo-mutants. With an increase of chloride concentration from 0 to 140 mM, the rate constants of iron uptake decrease slightly for the wild-type apo-hTF/2N and the apo-H249A mutant (∼15%), moderately for the apo-H249Q mutant (∼56%) and sharply for the apo-H249E mutant (∼72%).

DISCUSSION

Spectral Characteristics of Mutant Proteins. Histidine 249 is located at the hinge point of the two domains which acts as the pivot for the "see-saw"-like motion between open and closed conformations of hTF/2N. In iron-loaded hTF/2N, His 249 binds to the iron center and also links to the second-shell residue, Glu 83, through a water molecule (*8*). In apo-hTF/2N, His 249 is an important second-shell residue in the network hydrogen bonded to Glu 83 (*11*). It was expected that mutation of such a critical residue would result in a profound effect on the iron-binding properties of the protein. This is immediately indicated by the absorption spectra of the three histidine mutant proteins with the absorbance band in the visible range blue-shifting 15, 30, and 45 nm, respectively, for the carbonate complexes of the H249E, H249Q, and H249A mutants. Other mutants containing mutations at ligands Asp 63 and Tyr 95 also feature similar large blue-shifts in the visible spectra, reflecting strong interaction between iron and the tyrosine ligand(s) and characterized by weak iron-binding (*12*, *13*). In the case of the histidine mutants, H249A has the weakest iron-binding ability, such that passage over the gel filtration column removes half of the iron from the protein. However, it is noteworthy that the iron-binding ability is not totally abolished as found for the Y188F mutant where lack of the ligand Tyr 188 led to complete absence of the normal carbonate complex (*13*). Impaired iron-binding ability has also been found in the equivalent histidine mutants of lactoferrin (*21*).

Replacement of the histidine ligand in the H249A and H249Q mutants results in a preference of the proteins for NTA as synergistic anion. This may due to the ability of NTA to provide an additional pendant ligand. The NTA complexes have similar absorption spectral characteristics to wild-type Fe-hTF/2N−CO_3 and are kinetically much more stable than the corresponding carbonate complexes (see below).

The striking differences in the EPR spectra between wild-type hTF/2N and the histidine mutants also reveal the dramatic effect of the mutations (Figure 1). In a manner similar to other mutant proteins including D63A and Y95F which contain three amino acid ligands (*12*, *13*), the H249A and H249Q mutants have pure rhombic EPR spectra. The treatment with NTA leads to the absence of the small features but does not change the major rhombic signal. This confirms that NTA binds to the metal but indicates that the binding does not dramatically change the appearance of the spectrum. On the basis of the above absorption and EPR spectra, we speculate that the Gln 249 in the H249Q mutant does not directly bind to the iron center but indirectly affects the overall iron binding. Perhaps, a water molecule fills the coordination position of the normal histidine ligand and bridges between the iron center and the Gln 249 in the H249Q mutant. This could also provide an explanation for the observation that the Fe-H249Q−CO_3 complex is orange but the Fe-H249A−CO_3 complex is yellow (Table 1).

In contrast, structural analysis confirms that in the H249E mutant the Glu 249 bonds to the iron as well as to Lys 296, resulting in the disruption of the "dilysine K206-K296 trigger" (*22*, *23*). The EPR spectrum of the H249E mutant is significantly different from those for both wild-type hTF/2N and the other histidine mutants as has been reported (Figure 1) (*24*). This can be accounted for by the fact that the iron binding is perturbed by the introduction of the negative ligand, Glu 249, to replace the neutral ligand, His 249. The substitution of an oxygen from Glu for a nitrogen from His in binding to the iron may well contribute to the unusual appearance of the EPR spectra of the H249E mutant. In the presence of NTA, the iron in the H249E mutant is bound to a mix of carbonate and NTA with the carbonate complex representing ~94% of the total. Obviously, after multiple treatments of the protein with buffer containing NTA, a small amount of NTA is present in the iron binding in the H249E mutant which is not enough to observe in the absorption spectrum. A similar complex mixture has been reported by Aisen et al. for an oxalate-native transferrin complex (*25*).

Anion-Exchange Reaction. For the H249A and H249Q mutants, the conversion between their carbonate and NTA complexes can be observed by absorption spectroscopy since the two forms have λ_{max}s that are far enough apart. Similar to the situation for other mutants such as D63S (*12*) and R124A (*10*), the existence of an intermediate in this conversion is suggested through absorption spectra monitored during titration with a replacement of anion of the corresponding complex. With an absorbance stopped-flow spectrometer, we now are able to identify the intermediate and measure the rate constants for the conversions between both ternary anion complex forms.

As shown in Figure 2, the conversion between the carbonate and NTA complexes of mutant H249A involves two steps, the addition of the anion to the starting ternary complex to form an intermediate and the generation of the final product, with the first step going much faster than the second. This is true in either direction. The preference of the mutant protein for NTA is confirmed by the facts that the formation of the NTA complex is more than 15 times faster than the formation of the carbonate complex and that much more bicarbonate is required to reach a similar pseudo first-order rate constant k_1. Overall, the conversion reaction can be expressed as follows:

$$\text{Fe-H249A-(A)} + \text{B} \overset{k_1}{\leftrightarrow} \text{Fe-H249A-(A,B)} \overset{k_2}{\leftrightarrow} \text{Fe-H249A-(B)} + \text{A}$$

where A and B are the anions, carbonate, or NTA. A detailed kinetic analysis of these exchange phenomena will be published separately.

Iron Release and Uptake. As mentioned above, the participation of Glu 249 instead of His 249 in the iron coordination in the H249E mutant disturbs the iron binding of the protein. This may be due to the fact that Glu 249 brings in an extra negative charge that interrupts the original charge balance in the binding site. Furthermore, the substitution of His 249 with Glu 249 perturbs the second shell network and breaks the dilysine trigger by forming a salt bond between Glu 249 and Lys 296 (*22*). According to the result of our study with the Lys 206 and Lys 296 mutants (*16*), the loss or interruption of the dilysine trigger results in slow iron release from the protein. In the H249E mutant, this increased kinetic stability appears to be counterbalanced by an unfavorable overall iron binding involving Glu 249. The observed ~3-fold faster iron release from the Fe-H249E mutant compared to wild-type Fe-hTF/2N can be considered to be the sum of these opposing effects. Nevertheless, the H249E mutant is still kinetically much more stable than the other histidine mutants, H249A and H249Q, since these latter mutants provide no substitute ligand for the iron. Given the fact that the iron release rates for the H249Q mutant are the same order of magnitude as those for the H249A mutant, it can be assumed that the H249Q mutant has also lost an iron-binding ligand, a reasonable inference reinforced by its spectral characteristics. Zak et al. reported that another histidine mutant, H249Y, releases iron at a fast rate (*26*). We predict that the Tyr 249 in the H249Y mutant also does not directly coordinate the iron center.

The vast difference in the iron-release rates between the carbonate and NTA complexes of the H249A and H249Q mutants again shows that the mutant proteins favor NTA, which can contribute one more ligand donor group to fill the vacancy left by the absent His 249. This also explains why the iron uptake rate for the H249A is only slightly decreased and why the rate for the iron uptake by mutant H249Q is even higher than that for wild-type hTF/2N (Table 4). It is clear that both the H249A and H249Q mutants form the NTA complexes during iron uptake under the present conditions, as indicated by their $\lambda_{max} \approx 472$ nm after reaction is complete.

The chloride effect on the iron release from the histidine mutant proteins resembles our previous observation with other Fe-hTF/2N mutants and allows a similar explanation to be given (*19*). At neutral pH, chloride retards iron release from stable iron-binding proteins by competing with the chelator for the anion-binding site(s) near the iron center and accelerates iron release from very weak iron-binding proteins

by directly removing iron from the proteins. Given the fact that iron removal from Fe-H249E is only three times faster while Fe-H249A−NTA and Fe-H249Q−NTA are more than 150 times faster than the wild-type protein, we place the H249E mutant into the stable iron-binding category and the H249A and H249Q mutants into the weak binding category.

The chloride effect on iron uptake closely relates to the anion binding to the apo-proteins. Lys 296, the major anion-binding residue (*16*), is H-bonded to Glu 249 in Fe-H249E (*22*). It is therefore reasonable to presume, based on their opposite charge properties, that, in apo-H249E, Glu 249 would interact with Lys 296, thereby muting the anion-binding ability of the Lys 296 residue. This is the reason we do not observe the typical anion binding between sulfate and apo-H249E (Table 3). It is also possible that Gln 249 in apo-H249Q is weakly H-bonded to Lys 296 resulting in weaker anion binding with a lower $\Delta\epsilon$. The slightly weaker sulfate binding with an unchanged $\Delta\epsilon$ for apo-H249A suggests that the substitution of His 249 with Ala has little effect on Lys 296.

The anion-binding properties of the histidine mutants correspond very well to the chloride effect on the iron uptake behavior of the proteins. The parallel relationship between chloride and sulfate in anion binding to apo-transferrin has been documented (*16*). Chloride retards the iron uptake in the order, in terms of extent, H249E > H249Q > H249A ≈ hTF/2N, resembling in reverse the anion binding ability, apo-H249E ≪ apo-H249Q < apo-H249A ≤ apo-hTF/2N. The retarding effect of chloride appears to occur by a competition between chloride and the "synergistic anion" (carbonate or NTA in these cases) for an anion-binding site near the metal binding center. This implies that Lys 296 could also be one of the initial anion-binding site(s) for the synergistic anion which then moves to the position with Arg 124 upon iron binding.

Conclusion. A substantial impact on the iron-binding properties of the transferrin N-lobe has been found when the His 249 ligand is mutated to Glu, Ala, or Gln. The effect of the mutations can be observed via the comparison between wild-type and the mutant proteins in their absorption and EPR spectra, anion-binding, and iron-binding and iron-release behaviors. The substitution of His 249 with Glu results in relatively weak iron binding of the protein, although the Glu is still a binding ligand for iron. In the apo-H249E protein, the negatively charged Glu 249 appears to interact with the positive second-shell residue Lys 296 which then is unavailable for anion binding, leading to a significant chloride effect. Mutating the histidine to alanine or glutamine eliminates the binding ability of the histidine ligand, so that the resulting mutants H249A and H249Q are kinetically much more labile than the parent protein. The absence of the histidine ligand also leads to a preference of the H249A and H249Q mutants for NTA in iron binding because of the additional liganding group provided by NTA. The carbonate and NTA complexes are interconvertible; an intermediate species is identified for the conversion. Overall, disabling the histidine ligand does not completely abolish the iron-binding ability of hTF/2N, a finding consistent with the situation in lactoferrin (*21*).

ACKNOWLEDGMENT

We thank Mr. John K. Grady for assistance with some of the sample preparations and EPR measurements.

REFERENCES

1. Harris, D. C., and Aisen, P. (1989) in *Iron Carriers and Iron Proteins* (Loehr, T. M., Ed.) pp 239−351, VCH Publishers, Inc, New York.
2. Chasteen, N. D., and Woodworth, R. C. (1990) in *Iron Transport and Storage* (Ponka, P., Schulman, H. M., and Woodworth, R. C., Eds.) pp 67−79, CRC Press, Boca Raton, FL.
3. Baker, E. N. (1994) *Adv. Inorg.Chem. 41*, 389−463.
4. Anderson, B. F., Baker, H. M., Dodson, E. J., Norris, G. E., Rumball, S. V., Waters, J. M., and Baker, E. N. (1987) *Proc. Natl. Acad. Sci. U.S.A. 84*, 1769−1773.
5. Bailey, S., Evans, R. W., Garratt, R. C., Gorinsky, B., Hasnain, S. S., Horsburgh, C., Jhoti, H., Lindley, P. F., Mydin, A., Sarra, R., and Watson, J. L. (1988) *Biochemistry 27*, 5804−5812.
6. Kurokawa, H., Mikami, B., and Hirose, M. (1995) *J. Mol. Biol. 254*, 196−207.
7. Zuccola, H. J. (1993) *The crystal structure of monoferric human serum transferrin*, Thesis/Dissertation, Georgia Institute of Technology, Atlanta, GA.
8. MacGillivray, R. T. A., Moore, S. A., Chen, J., Anderson, B. F., Baker, H., Luo, Y., Bewley, M., Smith, C. A., Murphy, M. E. P., Wang, Y., Mason, A. B., Woodworth, R. C., Brayer, G. D., and Baker, E. N. (1998) *Biochemistry 37*, 7919−7928.
9. Woodworth, R. C., Mason, A. B., Funk, W. D., and MacGillivray, R. T. A. (1991) *Biochemistry 30*, 10824−10829.
10. Li, Y., Harris, W. R., Maxwell, A., MacGillivray, R. T. A., and Brown, T. (1998) *Biochemistry 37*, 14157−14166.
11. Jeffrey, P. D., Bewley, M. C., MacGillivray, R. T. A., Mason, A. B., Woodworth, R. C., and Baker, E. N. (1998) *Biochemistry 37*, 13978−13986.
12. He, Q.-Y., Mason, A. B., Woodworth, R. C., Tam, B. M., Wadsworth, T., and MacGillivray, R. T. A. (1997) *Biochemistry 36*, 5522−5528.
13. He, Q.-Y., Mason, A. B., Woodworth, R. C., Tam, B. M., MacGillivray, R. T. A., Grady, J. K., and Chasteen, N. D. (1997) *Biochemistry 36*, 14853−14860.
14. Nelson, R. M., and Long, G. L. (1989) *Anal. Biochem. 180*, 147−151.
15. Funk, W. D., MacGillivray, R. T. A., Mason, A. B., Brown, S. A., and Woodworth, R. C. (1990) *Biochemistry 29*, 1654−1660.
16. He, Q.-Y., Mason, A. B., Tam, B. M., MacGillivray, R. T. A., and Woodworth, R. C. (1999) *Biochemistry 38*, 9704−9711.
17. Mason, A. B., Tam, B. M., Woodworth, R. C., Oliver, R. W. A., Green, B. N., Lin, L.-N., Brandts, J. F., Savage, K. J., Lineback, J. A., and MacGillivray, R. T. A. (1997) *Biochem. J. 326*, 77−85.
18. He, Q.-Y., Mason, A. B., Woodworth, R. C., Tam, B. M., MacGillivray, R. T. A., Grady, J. K., and Chasteen, N. D. (1998) *J. Biol. Chem. 273*, 17018−17024.
19. He, Q.-Y., Mason, A. B., and Woodworth, R. C. (1997) *Biochem. J. 328*, 439−445.
20. Cheng, Y. G., Mason, A. B., and Woodworth, R. C. (1995) *Biochemistry 34*, 14879−14884.
21. Nicholson, H., Anderson, B. F., Bland, T., Shewry, S. C., Tweedie, J. W., and Baker, E. N. (1997) *Biochemistry 36*, 341−346.
22. MacGillivray, R. T. A., Bewley, M. C., Smith, C. A., He, Q.-Y., Mason, A. B., Woodworth, R. C., and Baker, E. N. (2000) *Biochemistry 39*, 1211−1216.
23. Dewan, J. C., Mikami, B., Hirose, M., and Sacchettini, J. C. (1993) *Biochemistry 32*, 11963−11968.
24. Grady, J. K., Mason, A. B., Woodworth, R. C., and Chasteen, N. D. (1995) *Biochem. J. 309*, 403−410.
25. Aisen, P., Aasa, R., Malmstrom, B. G., and Vanngard, T. (1967) *J. Biol. Chem. 242*, 2484−2490.
26. Zak, O., Aisen, P., Crawley, J. B., Joannou, C. L., Patel, K. J., Rafiq, M., and Evans, R. W. (1995) *Biochemistry 34*, 14428−14434.

BI9915216